20th International Conference on Renewable Energies and Power Quality (ICREPQ'22)
Vigo (Spain), 27th to 29th July 2022
Renewable Energy and Power Quality Journal (RE&PQJ)
ISSN 2172-038 X, Volume No.20, September 2022

Comparison of Bang Bang and PMW switching techniques for DC/AC photovoltaic converter

A. MARTINEZ[1], Y. KRIM[2], D. ABBES[2] and B. EKER[1]

[1] Laboratoire Energie Renouvelable Propre & Alternative
EIGSI, 26 rue de vaux de Foletier, 17041
La Rochelle Cedex France
andre.martinez@eigsi.fr, Tél. : +33 546458045

[2] Univ. Lille, Arts et Metiers Institute of Technology, Centrale Lille, Junia, ULR 2697 – L2EP, F-59000 Lille, France
dhaker.abbes@junia.com, Tél. : +33 328384858
youssef.kraiem@junia.com, Tél. : +33 642978366

Abstract. The general objective of this paper is to demonstrate that simple control strategy can be implemented in photovoltaic (PV) systems. A complete PV installation is embedded under MATLAB/Simulink environment to simulate and compare two control methods. The first one is based on bang bang control (Hysteresis) and the second one is the pulse width modulation method. We are focussing in applying these simple control strategies in the case of PV system operating in a standalone mode supplying an AC load. The integration with the load is made by a "H bridge". Specific goals are mastering and realising the complete model of the PV installation and its control algorithm (PV array, AC-DC converter, maximum power point tracking ...). Control strategies have been developed and simulated to visualise the functionality and convenience of the different control schemes of the PV system. Simulation results allow the comparison of the different control techniques with a particular attention for two criteria: the total efficiency as well as the harmonic distortion rate. Results shows that simple bang bang algorithm gives better results in terms of efficiency and harmonic distortion rate.

Key words. PV systems, control strategies, total efficiency, total harmonic distortion.

1. Introduction

It is no longer necessary to demonstrate the interest of renewable energy sources to replace fossil energies and thus, to reduce the environmental impact as well as energy dependence. From different sources, it is possible to produce electricity, but not only (It is possible to produce heat also). Photovoltaic (PV) systems, specifically, have a growing interest and renewable energies, with this source, is constantly increasing among the others. It's present all over the world. Many projects and research are conducted for over twenty years now at least. Of course, this energy has disadvantages such as fluctuating character and the fact that the PV "sensor" has a low efficiency. However, the research will make it possible to increase considerably this performance. Since the invention of the PV cell in 1954, this technology has been developed continuously. The efficiency of the first PV cell was 5 %. Currently in laboratories, it is possible to achieve efficiencies higher than 40 % [1]. Recently, PV energy became more and more important. Consequently, because of the globalisation and permanent increase of the world's population, more and more energy is required. PV energy is a proper alternative compared with conventional electrical energy production and one option to solve future energy problems. The potential of PV application is enormous. A surface of about 64.500 km^2 in the Sahara Desert would theoretically be sufficient to cover the global energy demand [2].

One key to make this technology profitable is improving the efficiency. There are multiple scientific disciplines that concern PV technology, e.g., semiconductor physics and material sciences for the PV cell itself and multiple areas of activities concerning electronics. One field of electronics is electronic command and control. Electronic command and regulation in a PV system must ensure that the PV cell operates at its maximum power point knowing by the terminology Maximum Power Point Tracking (MPPT) and provide the best possible adaptation of power electronic components [3]. The power of PV systems depends in part on PV irradiation and temperature. As a result, the power generated by PV systems is not guaranteed and may vary; this is the reason why storage solutions have been addressed [4], but not addressed in this paper.

In this paper, we are interested in applying two control strategies in the case of PV system connected to an AC load. The first control technique is based on a bang bang control system. The second one uses a PMW method to generate the control signals for the converter used to connect the PV infrastructure to the power consumer. In the first part, we establish the model of the PV cell. Then, we detail the MPPT as well as the DC/AC converter and the different types of performances to be considered. In the third part, after choosing the electrical topology of the

PV system, we compare two control strategies for the inverter. The system architecture is based on a "H bridge" with connection to the load. The simulation results make it possible to compare the various control techniques especially on the following points: the total efficiency as well as the harmonic distortion rate.

2. PV Cell Characterization

PV cell models have been already investigated by researchers [5, 6]. The model presented in Fig. 1 is frequently used by the scientific community. A current generator with a behavior equivalent to a current source shunted by a diode is described

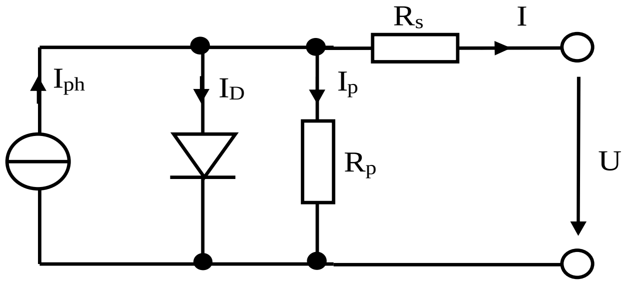

Fig. 1. PV generator model with a single diode and two resistors

The PV cell's intern conductors generate a fall of voltage inside, due to the serial resistance R_S. Losses within the semiconductor and leakage current is occurring. These losses are represented by the parallel resistance R_P. PV cell's equivalent scheme can be written mathematically (1).

$$0 = I_{PH} - I_D - I_P - I \tag{1}$$

with:

$$I_P = \frac{U_D}{R_P} = \frac{U + I \cdot R_S}{R_P} \tag{2}$$

Thus, (3) can be found for the equivalent schematic of a PV cell whereas I is the PV cell's output current.

$$0 = I_{PH} - I_D \cdot \left(\exp\left(\frac{U_D + I \cdot R_S}{m \cdot U_T}\right) - 1\right) - \frac{U_D + I \cdot R_S}{R_P} - I \tag{3}$$

with:

I_{ph} is the photovoltaic current due to irradiation. If the panel is composed of Np cells connected in parallel, then $I_{ph} = I_{ph\ cell} \times N_p$ where $I_{ph\ cell}$ is the saturation current for a single cell;

I_D is the saturation current of the PV panel. $I_D = I_{D\ cell} \times N_p$ where $I_{D\ cell}$ is the current of a single cell and Np the number of cells in parallel;

Ut: thermal potential of the panel. $U_t = \frac{N_S \times K \times T}{q}$, Ns is number of cells in series, K: Boltzmann constant, q charge of an electron and T temperature of the p-n junction. T is assumed equal to the ambient temperature;

m: ideal constant of the diode, assumed equal to 1 in our case:

U: voltage across the panel.

As (3) is an implicate one, it is only possible to solve them using numerical methods. A common practise to solve those equations is the Newton-approximation.

Applying the Newton approximation on (3), (4) can be found for the output current I_i.

$$I_{i+1} = I_i - \frac{I_{PH} - I_D \cdot \left(\exp\left(\frac{U + I_i \cdot R_S}{m \cdot U_T}\right) - 1\right) - \frac{U + I_i \cdot R_S}{R_P} - I_i}{-\frac{I_S \cdot R_S}{m \cdot U_T} \cdot \exp\left(\frac{U + I_i \cdot R_S}{m \cdot U_T}\right) - \frac{R_S}{R_P} - 1} \tag{4}$$

3. Investigated Control Strategies

Technologies for controlling PV system are already very advanced, especially for PV plants. The two most influenced parts of modern controlling are the MPPT and the DC-AC inverter.

A. MPPT strategy

Many MPPT techniques have been proposed in the literature. Incremental conductance algorithm and perturb and observe algorithm are among most popular. In our paper, our technique is based on the first one, even if the main weakness of this algorithm is its complexity in comparison with the perturb and observe algorithm. At a glance, the Incremental conductance can establish with a good accuracy that the MPPT has reached the MPP and stop perturbing the operating point. If this condition is not met, the direction in which the MPPT operating point must be perturbed can be calculated using the relationship between dI/dV and –I/V

The efficiency of modern MPPT strategy is generally high (up to 99 percent [7]). Fig. 2 shows evolution of the current and power of the studied PV installation as function of the PV output voltage.

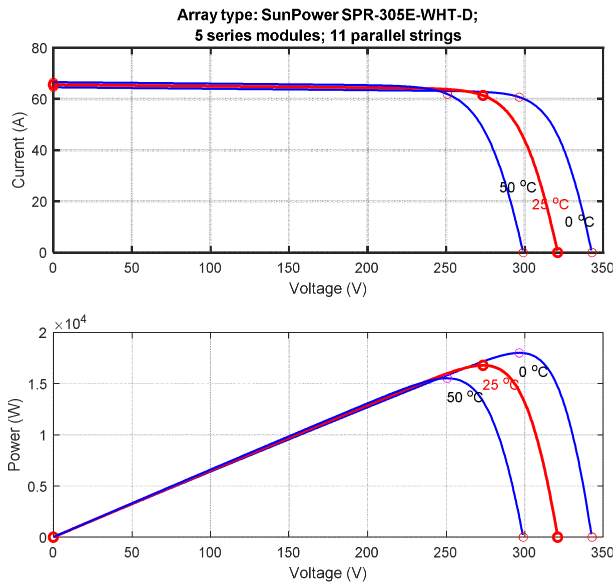

Fig. 2. PV current and power versus the PV output voltage.

Thus, the maximum power for a PV cell is reachable. This concept presents the basis of the MPPT terminology. The voltage U_{MPP} is smaller than the off-load voltage and the short circuit current is higher than I_{MPP}. Mathematically U_{MPP} and I_{MPP} can be obtained by resolving (3) to U_{MPP} and I_{MPP}, according to (5) and (6) (neglecting the influence of the parallel resistor).

$$I_{MPP} = I(U_{MPP}) = I_K - I_S \cdot \left(\exp\left(\frac{U_{MPP}}{m \cdot U_T} \right) - 1 \right) \quad (5)$$

$$U_{MPP} = U_L - m \cdot U_T \cdot \ln\left(1 + \frac{U_{MPP}}{m \cdot U_T} \right) \quad (6)$$

As (6) is non-linear it must be solved numerically, according to the Newton approximation. Furthermore, the MPPT can be computed using the derivation of the PV cell's power curve. The maximum of the PV cell's power curve (derivation=0, maximum power) can be calculated according to (7).

$$\frac{dP(U_{MPP})}{dU} = \frac{d(U_{MPP} \cdot I(U_{MPP}))}{dU} = I(U_{MPP}) + U_{MPP} \cdot \frac{dI(U_{MPP})}{dU} = 0 \quad (7)$$

The power P_{MPP} in the operation point MPPT can be calculated according to (8).

$$P_{MPP} = U_{MPP} \cdot I_{MPP} < U_L \cdot I_K \quad (8)$$

with:
U_L the off-load voltage with I=0 (Fig. 1) and I_K the short circuit current.
If a solar cell is short circuited, the short circuit current I_K corresponds nearly to the photo current I_{PH}. The more the temperature is high, the more the short circuit current increases.
Also, the MPPT power has a temperature coefficient. The equation to calculate P_{MPP} depending on the temperature is analogue to (9).

$$I_K(\vartheta_2) = I_K(\vartheta_1) \cdot \left(1 + \alpha_{1K} \cdot (\vartheta_2 - \vartheta_1)\right) \quad (9)$$

where $\vartheta_{1\ and\ 2}$ are the temperature at initial condition and final one respectively, and α_{1K} is the coefficient temperature.
The more the temperature is high, the more the short circuit current increases. Normally the current's temperature coefficient is between $\alpha_{1K} = +10^{-3}/°C$ and $\alpha_{1K} = +10^{-4}/°C$.

For the MPPT, power temperature coefficient is negative and for Silicium PV cells the value is between $\alpha_{PMPP} = -3 \cdot 10^{-3}/°C$ and $\alpha_{PMPP} = -6 \cdot 10^{-3}/°C$. A temperature increases of 25°C provokes a power diminution of 10%. In datasheets, the MPPT is given according to STC (Standard Test Conditions) conditions and normal given in W_p (Watt-peak).
From time to time, there are new technologies to perform the MPPT [8]-[9]. This article is nevertheless not focused on MPPT.

B. DC-AC inverter

A DC-AC inverter equipped with hard switches (switches that are turned off without applying zero voltage switching), provide an efficiency of around 95 to 96 percent. In this article, a DC-AC inverter with soft switching was carried out, which increase the efficiency up to 97 to 98 percent [10].
PV-inverter is the junction between the PV-array and the power consumer (load) where the PV energy is directly injected in. Furthermore, it is possible to supply PV energy into local electricity grid, e.g., a house and to supply the excessive energy into the public electricity grid.
For PV installations up to 5 kW, single phase is used. For higher power, the alimentation can be done in three-phase. There are two ways for three-phase supply, the first one is based on a three-phase DC-AC inverter and the second one is to apply three single phase DC-AC inverters that supply symmetrically into the electricity grid.
Modern inverters for PV systems can match the following demands:

- Conversion of the PV generator's direct parameters (voltage and current) into alternating parameters according to the public electricity grid (voltage, frequency);
- Quick adaptation of the MPPT according to exterior conditions (PV irradiation, temperature);
- Saving and visualisation of data, e.g., power, voltage and current;
- Resistance against over voltage, reverse polarity, overpower;
- Match standardisation demands of electrical institutions.

Fig. 3 shows the architecture of a PV conversion system with a DC/AC inverter.

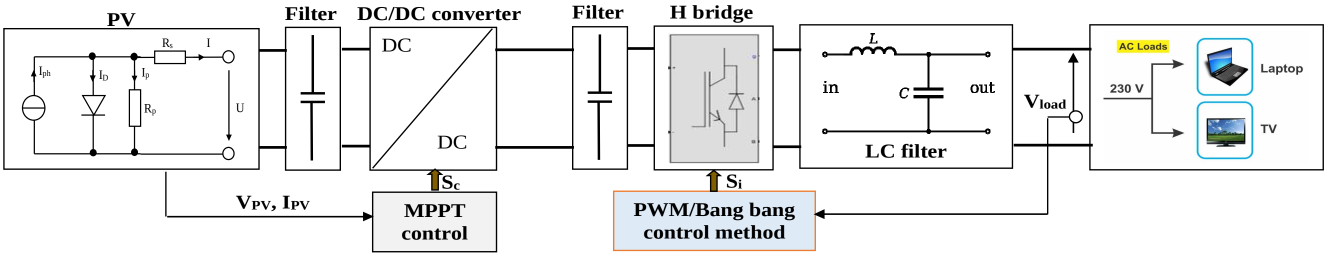

Fig. 3. Connection interface of a PV installation to the power grid or load based on DC/AC converter.

The following paragraphs describe the PV inverter's single components.

The heart of a PV inverter is the DC-AC inverter. It must be distinguished between line commutated and selfcommutated inverters. The requirements for a DC-AC inverter are the following:

- delivering of alternating voltage and current with fixed frequency;
- having a good efficiency, even for loads below the nominal power;
- protection against short circuit current;
- less harmonic oscillation;
- over voltage protection.

Furthermore, one of the objectives of this article is to show how different variations of a switch control may influence the efficiencies and harmonic's behaviour. First, it should be started with a general PWM, comparing a triangular signal with a reference sinusoidal signal. Further simple bang bang controls were be found in [10] and one of them is investigated in this article. The objective is to compare these switch controllers and visualise the results.

4. Choice of typology of the PV System

To illustrate and to compare the different control strategies, a typology of the PV system must be chosen. The first decision that was made was to use either a grid connected, or non-grid connected system [11, 12]. Secondly, a structure with a large market segment was investigated, e.g., a low or medium power installation that can be implemented e.g., on roof tops of houses. As fabricants tend more and more to offer transformer less PV converter it is an interesting challenge to investigate such an installation. In this work, we decided to implement a standalone PV system to supply an AC load. Fig. 4 shows the architecture that was used throughout the work.

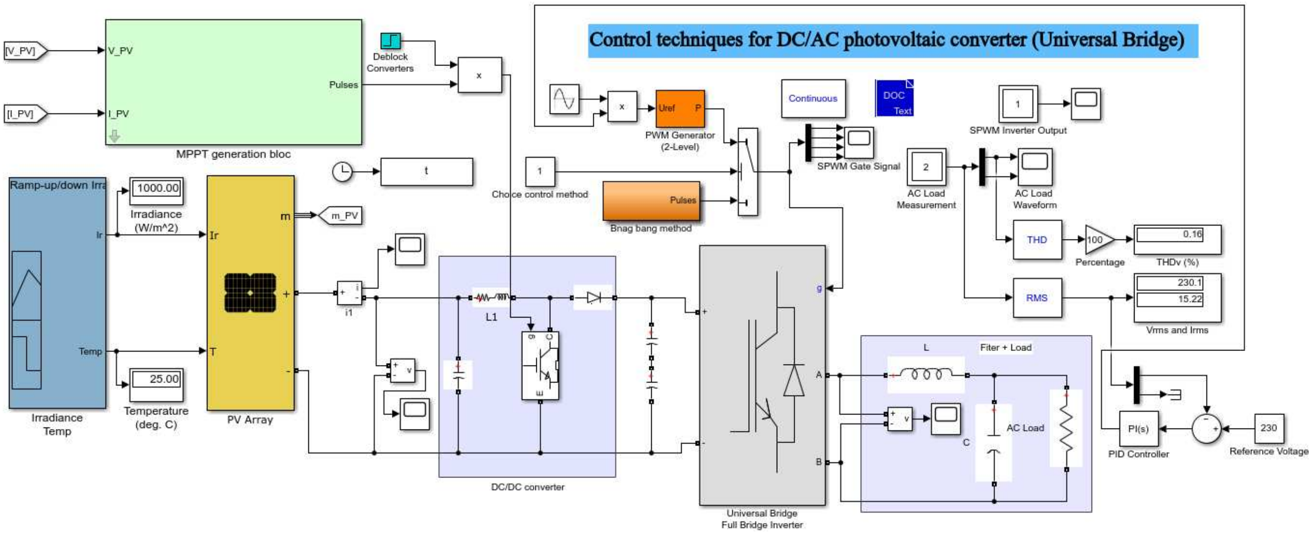

Fig. 4. Complete example application.

In this paragraph, results of different control strategies will be compared and visualised. Two control strategies have shown an adequate interest for investigations and are detailed after:

- Bang bang method;
- PWM sinus/triangle.

A. Introduction to the Bang Bang Regulation

As solution, is based on a bang bang regulator, an overview is done. Such a structure is based on a H bridge (Fig. 5). In this one, U_D is a direct voltage and U_{Mains} an AC voltage source. It is assumed that energy is injected into U_{Mains} [13, 14].

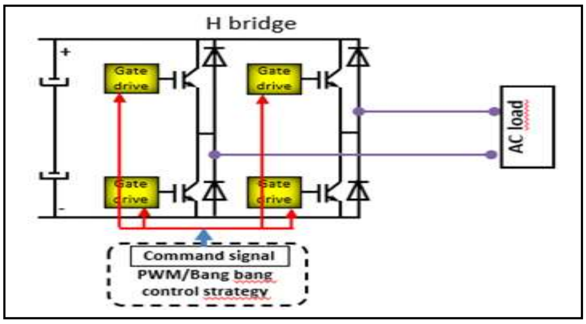

Fig. 5. H-bridge.

The bang bang regulation demands two different times depending on set point values. If e.g., a sinusoidal set point value without an offset is desired, the two set point values have to be as follows:

- One (sinusoidal) set point value must have a positive offset;
- The other one (sinusoidal) set point value must have a negative offset.

Fig. 6 shows graphically the desired curve (sinusoidal current) with its two set points. Furthermore, a typical measure (*I* measure in Fig. 6) is shown.

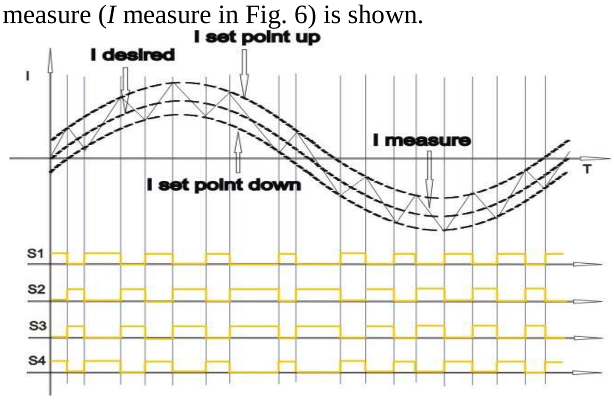

Fig. 6. Graphical illustration of the bang bang regulation.

Fig. 6 also visualises a basic switch control of a bang bang regulation. Assuming that S1 and S4 are switched on at any moment in Fig. 5, the current *I* measure (*i* in Fig. 5) is rising. As soon as the upper set point is achieved, S1 and S4 are switched off and S2 and S3 are switched on. This forces the current *i* in Fig. 5 to decrease. The decrease continues until the current reaches the downer set point value. As soon as *I* is inferior to the downer set point value S2 and S3 are switched off and S1 and S4 are switched on again. The current begins to augment again. The average v1alue of the resulting current is a sinusoidal shape as *I* desired in Fig. 6.

Remark: Fig. 6 shows the simplest version of a bang bang regulation. Practically this switch pattern would show inconvenience as all four switches are applied at the same time which would provoke a short circuit of the H-bridge (see Fig. 5) for a little while. The switching frequency depends on the gap between the upper and the downer set point value and the mains voltages on the inductance and resistance at the circuits output (L and R in Fig. 5). Further information about this kind of regulation can be found [15].

B. Bang Bang Method

The concept of the bang bang control strategy is summarized in Fig. 7.

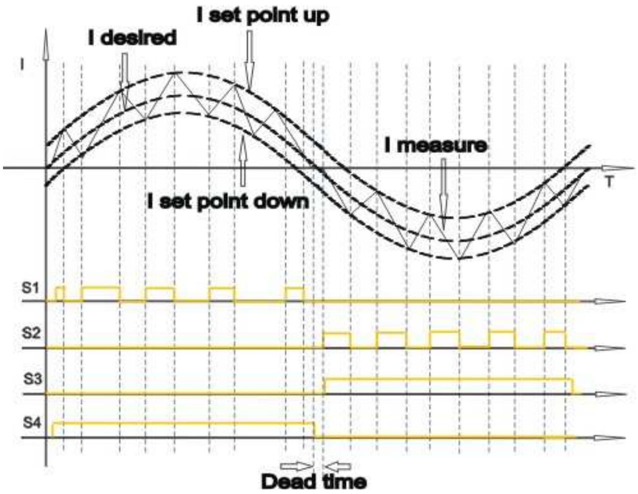

Fig. 7. Bang bang version overview switching scheme.

The desired current *I* that is injected into the AC load is sinusoidal as desired. The switching scheme to apply $S_{1,}$ $S_{2,}$ S_3 and S_4 in Fig. 5 to force the current to adapt the desired shape (sinusoidal) is also given with Fig. 7. During the positive part of the sinus wave the current increases when S_1 and S_4 are switched on at the same time. This also forces the current to flow through S_1 and $S_{4.}$ When the current has achieved an upper set point (*I* set point up in Fig. 7), S_1 is switched off. The inductance in Fig. 5 forces the current to continue and so the current flows through D_3 and $S_{4.}$ The AC load (U_{mains} in Fig. 5) operates as a charge that forces the current to decrease. As soon as the decreasing current undertakes the downer set point value (*I* set point down in Fig. 5) S_1 and S_4 are conducting again, and the procedure starts again. So, finally S_4 is switched on as long as the sinus wave is positive.

During the negative part of the sinus wave the current goes down when S_2 and S_3 are conducting at the same time which provokes a current flow through these two switches. If the current undertakes the negative set point (*I* set point down in Fig. 7) S_2 is switched off and the inductance forces the current to continue through S_3 and D_4. As the AC load operates as a charge, the current is increasing during the negative part of the sinus wave. As soon as the current is superior to the upper set point value, S_2 and S_4 are switched on again and the procedure starts again. Finally, it can be figured out that during the negative part of the sinus wave S_3 is conducting throughout the time. To prevent a short circuit during the transition between the positive and negative part of the sinus wave (I desired in Fig. 7) a little dead time is included where all switches are turned off.

The command signals S1, S2, S3, and S4 of the H bridge, generated by the developed band bang method, are depicted in Fig. 8.

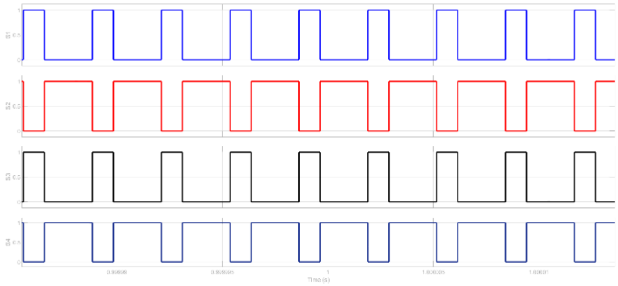

Fig. 8. Command signals of the H bridge generated by the bang bang method.

Fig. 9 presents the output voltage of the H bridge and the voltage and current that was supplied the AC load for the application “bang bang method”.

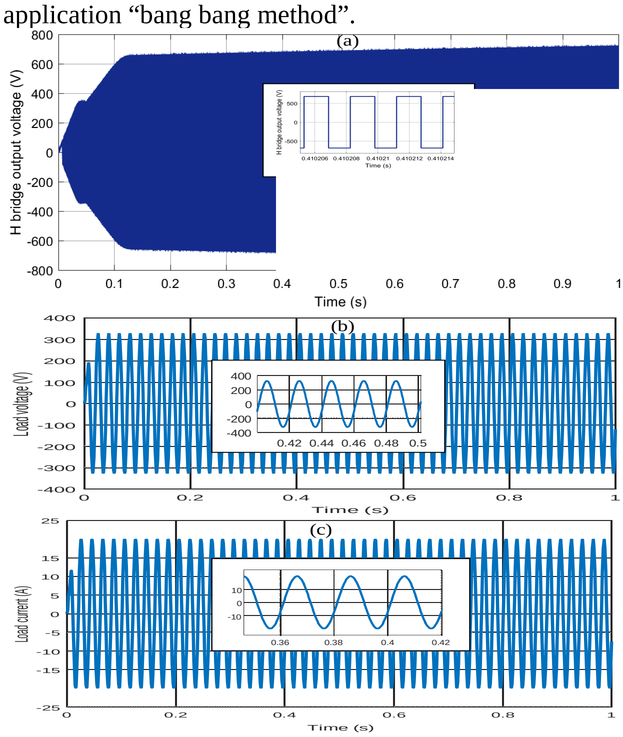

Fig. 9. Results of bang bang control method: (a) H bridge output voltage, (b) load supply voltage, (c) load supply current.

Generally, the performance of this regulator is quite satisfying. The values concerning the efficiencies are in compliance with PV converters that are currently on the market. The Total Harmonic Distortion (THD) for the bang bang method is low. Because of the limited step time (in all applications 10 µs) the switching frequency was not able to be increased. The limited step time of 10 µs is a compromise to have a satisfying switching frequency and an adequate simulation time. If the switching frequency had been chosen higher, the THD had been reduced again. A problem that provokes THD is the zero passing of the current. During a little while around the zero crossing all switches are turned off (see Fig. 7) to prevent a short circuit of the H-bridge. Another problem that causes THD are the bridge intern irregular currents that are created by the snubber circuits that are located parallel to the switches. It is very difficult to investigate them with Matlab/Simulink.

C. PWM method

Fig. 10 is used to give a brief introduction about the concept of the PWM modulation. Further information can be found in many articles such as [16].

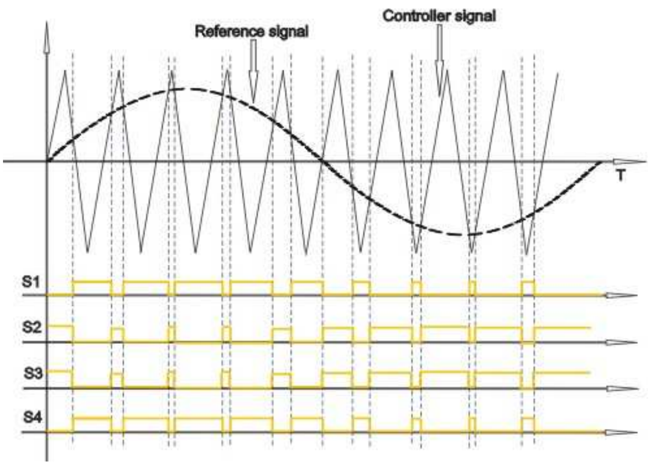

Fig. 10. Illustration of the PWM modulation.

The switches S1 and S4 as well as S2 and S3 in Fig. 5 are switched on and switched push pull. The triangular signal (controller signal) in Fig. 9 is compared with sinusoidal signal (reference signal). If the control signal is superior to the reference signal, S2 and S3 are switched on and if the triangular signal is inferior to the sinusoidal signal, S1 and S4 are switched on (Fig. 10). The created pulses have different widths; that's why this kind of switch control is called PWM. The individual switch configuration forces the current *i* in Fig. 5 either to increase or to decrease. The more the frequency of the control signal is high, the more the sinusoidal shape is precise. It is recommendable that the frequency of the control signal is a pair multiple of the reference signal's frequency. This prevents the occurrence of pair harmonics. The amplitude and frequency depend on the sinusoidal reference signal thus it is easy to modify the level and frequency of the output current.

In this context, the command signals of the H bridge created by the PWM strategy is presented in Fig. 11.

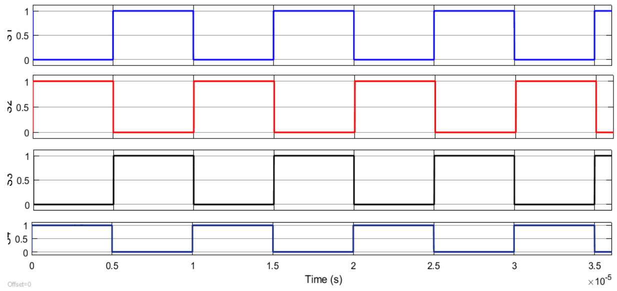

Fig. 11. Command signals of the H bridge generated by the PWM method.

Fig. 12 presents the voltage modulated by the H bridge, the supply load voltage, and the current that was injected into the load for the application "PWM method based on the comparison sinus/triangle".

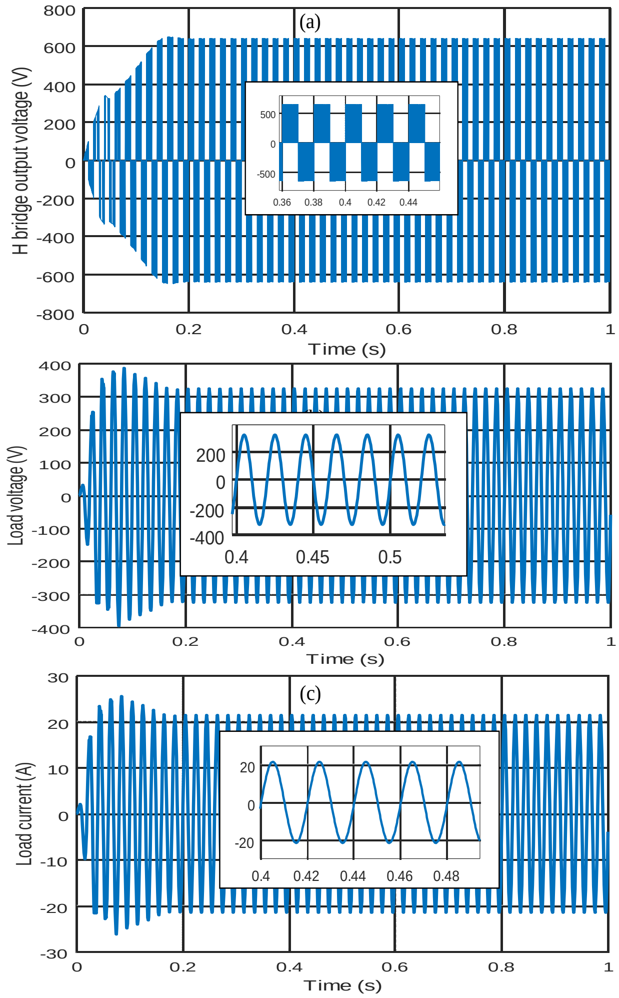

Fig. 12. Results of PWM control method: (a) H bridge output voltage, (b) load voltage, (c) current demanded by the load.

In this section, a comparative framework is discussed to show the difference between the bang bang control system and the PWM switch control method. As mentioned before, the H-bridge is short circuited for a little while during the switching is executed. This is the reason for the increased losses of 1.7 % within the H-bridge compared with the bang bang. Furthermore, there is an enormous increase of the THD (0.16 %). The set point value for the regulation is given by the MPPT. The regulated value is the output voltage of the equivalent schematic of the PV cell. So, the current value that is injected into the load controls this voltage. The phenomenon that occurred is the same than in described in the bang bang version: the amount of power that is injected into the load which is necessary to force the voltage to equal the set point cannot be delivered (sinusoidal) by the PV cell. Or otherwise said, the losses within the DC-AC converter are not considered within this regulation. Thus, the observed PWM modulation degree equaled 1.4 which automatically creates THD. However, first it was intended to improve the behavior by applying a variant, a further regulation circuit to adapt the set point value resembled to the switch controller “bang bang”. Practically, it would not have made sense as this kind of controller is normally not used for PV converters and so it was omitted.

Table I gives an overview about the measured electrical characteristics for the different switch control applications.

Table I. electrical results of the different commanding strategies.

ELECTRIC CHARACTERISTIC	BANG BANG	PWM
PV cell efficiency	0.1149	0.1149
Charging efficiency	0.95	0.94
Adaptation efficiency	0.99	0.99
Static efficiency	0.94	0.85
Total efficiency	0.1076	0.091
THD	0.017 %	0.16 %

5. Conclusion

The general objective of this article was to illustrate the improvement of the PV system efficiency by applying two control strategies, bang band and PWM method. The results for bang bang version are quite satisfying. The total efficiency of a PWM control system is in the region of 0.091. The total efficiency of the bang bang control strategy with the best performance is 0.1076. The PV cell efficiency is 0.1149 and so thanks to regulation strategies, around 94 % of the energy delivered by the PV array, is injected into the simulated AC load. We also demonstrated that simple control strategy can be implemented in such a PV system.

Matlab/Simulink is not the best appropriate tool to simulate switching procedures based on bang bang regulations. Considering that switching frequency of PV DC-AC converter is about between 20 and 500 kHz, simulation duration depends highly on the simulation step time, the simulation time would have been very low, and the duration time would have been huge. The consequence is that a simulated lower switching frequency has been applied. It is difficult to visualise the current behaviour. It would have been very interesting to envisage the results for the PV converter with zero-current-switching considering the created model.

According to the obtained results, the bang bang control method is a simple strategy with a very low THD compared to the PWM strategy, but its field of use is limited, where it is used to control the voltage. However, the converters are used, not only for the voltage control, but also for the control of powers and for high power systems. Thus, with the evolution of computing systems, the PWM strategy is preferred thanks to its robustness for the control of the active and reactive powers.

For future perspectives, different MPPT’s or others Bang bang version could be investigated and, DC-AC inverter topology e.g., a multilevel inverter. A regularly PWM generator applies its pulses to the H-bridge configuration and so it would be interesting to compare the H-bridges behaviour with a multilevel inverter, used for higher power.

Acknowledgements

This research has been commissioned and funded by the European PORTOS project (within the Atlantic Area Transnational Programme). The authors would like to thank the Atlantic program for their financial support in PORTOS project.

References

[1] Ahhad H. Alharbi, Sabre Kais, Theoretical limits of photovoltaics efficiency and possible improvements by intuitive approaches learned from photosynthesis and quantum coherence, Renewable and Sustainable Energy Reviews, Volume 43, 2015, Pages 1073-1089.

[2] Kurokawa, K. (Ed.). (2007). Energy from the Desert: Practical Proposals for Very LargeScale Photovoltaic Systems (1st ed.). Routledge.

[3] Madububa, B. I., Mbagwu, J. C., & Isiohia, D. O. (2020). Design, Construction, and Testing of Maximum Power Point Tracking (MPPT) Charge Controller for Photovoltaic (PV) Power Generation. Journal of Engineering Research and Reports, 17(1), 36-47.

[4] Belfedhal SA, Berkouk EM, Messlem Y (2019) Analysis of grid connected hybrid renewable energy system. Journal of Renewable and Sustainable Energy 11, 014702 (2019).

[5] Vergura, S. A Complete and Simplified Datasheet-Based Model of PV Cells in Variable Environmental Conditions for Circuit Simulation. Energies 2016, 9, 326.

[6] Abbes, D., Champenois, G., Martinez, A., & Robyns, B. (2013, October). Modeling and simulation of a photovoltaic system: An advanced synthetic study. In 3rd International Conference on Systems and Control (pp. 93-98). IEEE.

[7] Sven Killinger, David Lingfors, Yves-Marie Saint-Drenan, Panagiotis Moraitis, Wilfried van Sark, Jamie Taylor, Nicholas A. Engerer, Jamie M. Bright, On the search for representative characteristics of PV systems: Data collection and analysis of PV system azimuth, tilt, capacity, yield and shading, Solar Energy, Volume 173, 2018, 1087-1106.

[8] Hafsa Abouadane, Abderrahim Fakkar, Youssef Elkouari, David Ouoba, Performance of a new MPPT method for Photovoltaic systems under dynamic solar irradiation profiles, Energy Procedia, Volume 142, 2017, 538-544.

[9] Jazayeri, M. Uysal, S.; Jazayeri, K.”Evaluation of Maximum Power Point Tracking Techniques in PV Systems Using MATLAB/Simulink” Green Technologies Conference (GreenTech), 2014 Sixth Annual IEEE 2014 , Page(s): 54 – 60.

[10] J. Xi, Y. Chen, M. Chen, P. Chen and D. Xu, "A startup scheme for zero-voltage-switching PV inverter," 2015 IEEE Applied Power Electronics Conference and Exposition (APEC), 2015, 2333-2340.

[11] R. V. Dell Aquila, A new approach: Modelling, simulation,development and implementation of a commercial gridconnected transformerless PV inverter,”2010, pp. 1422-1429.

[12] Vinod, Raj Kumar, S.K. Singh, Solar photovoltaic modeling and simulation: As a renewable energy solution, Energy Reports, Volume 4, 2018, 701-712.

[13] Vinod, Raj Kumar, S.K. Singh, Solar photovoltaic modeling and simulation: As a renewable energy solution, Energy Reports, Volume 4, 2018, 701-712.
[14] M.A. Hasan, S.K. Parida, An overview of solar photovoltaic panel modeling based on analytical and experimental viewpoint, Renewable and Sustainable Energy Reviews, Volume 60, 2016, Pages 75-83.
[15] Naderipour A, AbdulMalek Z, Afrouzi HN, Ramachandaramurthy VK, Guerrero JM, A novel compensation current control method for grid-connected PV inverter to improve power quality in micro-grid. In: 2018 IEEE PES Asia-Pacific power and energy engineering conference (APPEEC), pp 143–148.
[16] Opiyo, N. (2016) Power Electronics for PV-Based Communal Grids. Smart Grid and Renewable Energy, 7, 67-82.